Depletion of CCR8⁺ Tumor Treg cells with SRF114 or Anti-CCR8 Therapy Promotes Robust Antitumor Activity and Reshapes the Tumor Microenvironment Toward a More Pro-inflammatory Milieu

Marisella Panduro, Yue Ren, Ricard Masia, Yu Yang, Andrew C. Lake, Vito J. Palombella, Jonathan A. Hill, James F. Mohan

Surface Oncology, Cambridge, MA, USA

SURFACE ONCOLOGY®

#5125

Background

- Foxp3⁺ regulatory T (Treg) cells play a crucial role in orchestrating immune responses across several tissues, including the tumor microenvironment (TME).[1,2]
- The dominant immune regulatory activity of Treg cells is evidenced, both clinically and preclinically, by the profound inflammatory dysregulation that arises in their absence.[1,2]
- CCR8 is a seven transmembrane G-coupled chemokine receptor protein. Its expression is predominantly upregulated on Treg cells in several types of tumors compared with peripheral blood and other lymphoid tissues.[3,4]
- CCR8⁺ tumor Tregs have been shown to have an activated phenotype and are highly suppressive *in vitro*.[3,4]
- Therapeutic antibodies targeting CCR8 have been developed to deplete tumor Treg cells. This represents an attractive strategy to reshape the local TME and enhance anti-tumor immune responses.[7-10]
- SRF114 is an afucosylated fully human IgG1 antibody that selectively targets human CCR8 (hCCR8) and induces depletion of CCR8⁺ Treg cells. SRF114 is currently in Phase 1 Clinical Studies (NCT05635643).

CCR8⁺ Tumor Tregs Are Highly Activated Cells with Potent Immune Suppressive Function

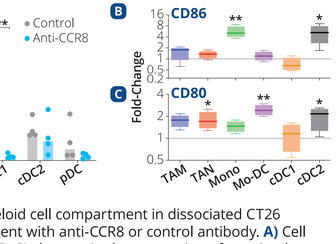

Anti-CCR8 Therapy Has Robust Anti-Tumor Activity in a Checkpoint-Resistant Melanoma Tumor Model

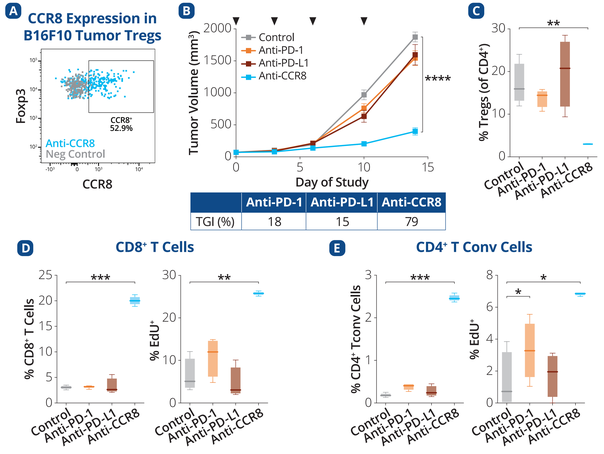

	Anti-PD-1	Anti-PD-L1	Anti-CCR8
TGI (%)	18	15	79

A) Representative graph of cytometric analysis of CCR8 expression on tumor Tregs measured in dissociated B16F10 tumors. **B)** Efficacy study evaluating anti-tumor activity of anti-CCR8, anti-PD-1, or anti-PD-L1 monotherapy treatments in the B16F10 tumor model. **C-E)** Cytometric analyses of tumor Treg cells and proliferating effector T cells from dissociated B16F10 tumors collected on Day 9 of study.

A) B16F10 tumors were collected on Day 13 after implantation and CCR8 expression was detected on Foxp3⁺ Treg cells by flow cytometry. B-E) Mice bearing subcutaneous B16F10 tumors were treated with anti-CCR8, anti-PD-1, anti-PD-L1, or control antibodies. B) Percent tumor growth inhibition (TGI, %) was calculated on Day 14 of study, (n = 10). C) Tumors were collected and the fraction of Foxp3⁺ Treg cells was determined (n=4). D-E) Mice were dosed with 1 mg 5-Ethynyl-2'-deoxyuridine (EdU) 24 hours prior to sample collection and fraction of EdU⁺ CD8⁺ effector T cells and EdU⁺ CD4⁺ Tconv cells were measured, respectively, (n = 4).

Anti-CCR8 Therapy Promotes Production of Proinflammatory Cytokines & Chemokines

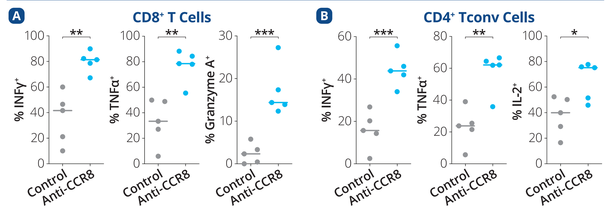

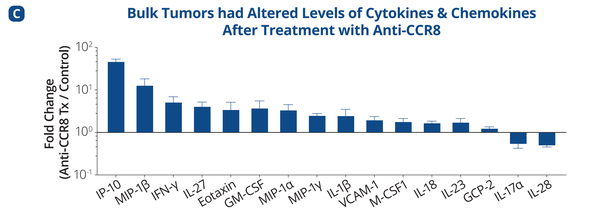

A-B) Resected tumor samples on Day 8 post-treatment initiation were restimulated *ex vivo* with PMA and ionomycin to evaluate intracellular cytokine levels of CD8⁺ T and CD4⁺ Tconv cells, respectively. **C)** Fold-change in cytokine levels evaluated in bulk tumor lysates.

Mice bearing B16F10 tumors were dosed with anti-CCR8 or control antibodies. A-B) Flow cytometric analyses of intracellular cytokine levels of TILs after *ex vivo* restimulation of dissociated tumors (n = 5). C) Levels detected by Luminex in snap-frozen and lysed bulk B16F10 tumors 4 days after treatment initiation with anti-CCR8 or control antibodies, (n = 4).

Abbreviations: ▼ = dosing day; APCs = antigen-presenting cells; cDC = conventional dendritic cell; CCR8 = C-C Chemokine Receptor 8; DC = dendritic cells; DF = diffusion dimension; dLN = draining lymph nodes; FFPE =formalin-fixed paraffin-embedded; Foxp3 = forkhead box P3 protein; hCCR8 = human CCR8; hCCR8KI = human CCR8 knock-in; IFNγ = interferon-gamma; IHC = immunohistochemistry; IL = interleukin; MO-DC = monocyte-derived dendritic cells; Mono = monocytes; NK = natural killer; PD-1 = programmed death 1; pDC = plasmacytoid dendritic cells; PMA = phorbol 12-myristate 13-acetate; TAM = tumor-associated macrophages; TAN = tumor-associated neutrophils; Tconv = conventional T cells; TGI = tumor growth inhibition; TIL = tumor-infiltrating lymphocytes; TME = tumor microenvironment; TNFα = tumor necrosis factor alpha; Tregs = regulatory T cells.

Statistics: * = p < 0.05; ** = p < 0.01; *** = p < 0.001; **** = p < 0.0001

References: 1) Plitas et al, *Ann Rev Can Biol* 2020. **2)** Sakaguchi et al, *Ann Rev Imm* 2020. **3)** Plitas et al, *Immunity* 2016. **4)** Wang et al, *Nat. Imm* 2019. **5)** Alvisi et al, *JCI* 2020. **6)** Whiteside et al, *Immunology* 2021. **7)** Campbell et al, *Can Res* 2021. **8)** Weaver et al, *OncoImm* 2022. **9)** VanDamme et al, *JITC* 2021. **10)** Kidani et al, *PNAS* 2022.

Anti-CCR8 and anti-PD1 Combination Therapy Enhances Overall Survival and Promotes Expansion of Effector T cells in B16F10 Melanoma

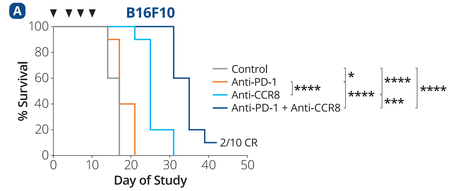

	Median Survival (Days)
Control	17
Anti-PD-1	17
Anti-CCR8	25
Anti-PD-1 + Anti-CCR8	35

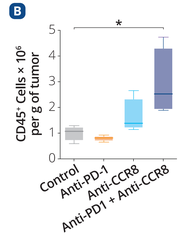

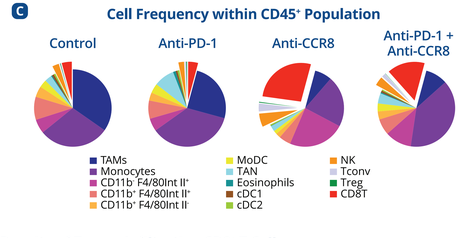

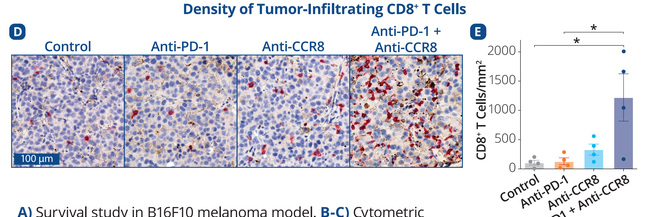

A) Survival study in B16F10 melanoma model. **B-C)** Cytometric analyses and average frequency, respectively, of TILs on Day 9 of study. **D)** Representative IHC images of infiltrating CD8⁺ T cells in B16F10 tumors on Day 9 of study. **E)** Quantification of density of infiltrating CD8⁺ T cells.

A) Mice bearing subcutaneous B16F10 tumors were treated with anti-CCR8, anti-PD-1, or control antibodies (n = 10). B) Total number of CD45⁺ cells per gram of tumor was measured by normalizing the total CD45⁺ cell count to tumor weight (n = 4). C) Frequencies of defined TILs were averaged per group and normalized to their total sum. D) IHC for CD8 using a red chromogen was performed on FFPE samples of tumors collected from the study. E) Infiltrating CD8⁺ T cells were quantified using image analysis on digitally scanned slides (n = 4).

Anti-CCR8 + Anti-PD-1 Combination Treatment Enhances Production of Pro-inflammatory Cytokines and Chemokines in Melanoma Tumors

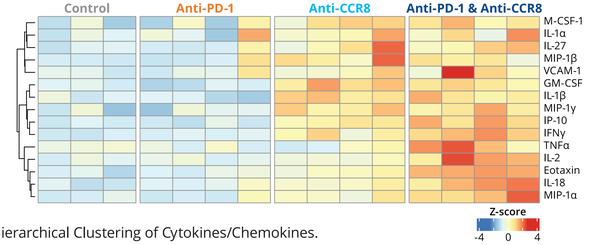

Hierarchical Clustering of Cytokines/Chemokines.

Detection by Luminex assay in snap-frozen and lysed bulk B16F10 tumors 8 days after treatment initiation. Tumor-bearing mice were dosed with anti-CCR8, anti-PD-1, a combination of both, or control antibodies, (n = 3-4).

Treatment with SRF114, a Fully Human Afucosylated IgG1 Antibody, Results in Robust Anti-Tumor Activity in Human CCR8 Knock-In Mice

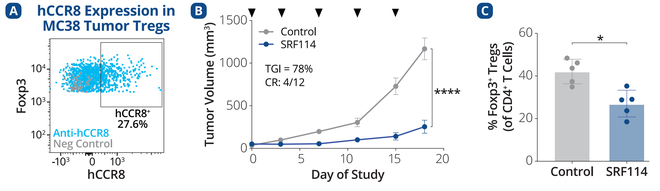

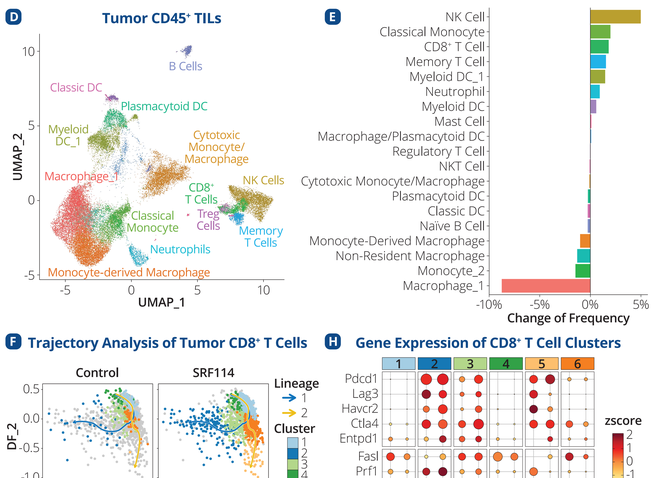

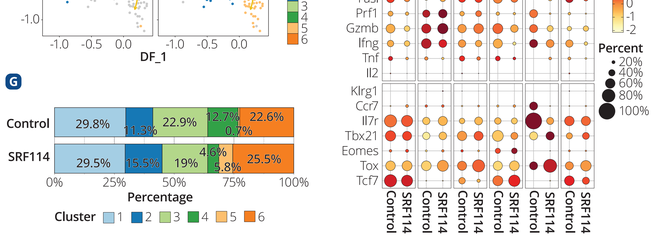

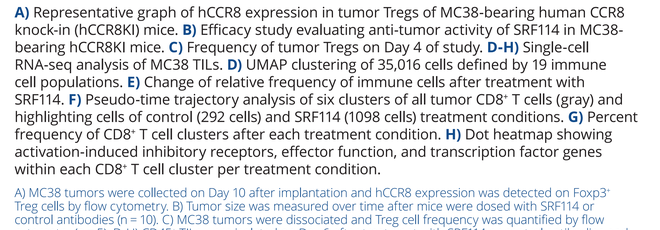

A) Representative graph of hCCR8 expression in tumor Tregs of MC38-bearing human CCR8 knock-in (hCCR8KI) mice. **B)** Efficacy study evaluating anti-tumor activity of SRF114 in MC38-bearing hCCR8KI mice. **C)** Frequency of tumor Tregs on Day 4 of study. **D-H)** Single-cell RNA-seq analysis of MC38 TILs. **D)** UMAP clustering of 35,016 cells defined by 19 immune cell populations. **E)** Change of relative frequency of immune cells after treatment with SRF114. **F)** Pseudo-time trajectory analysis of six clusters of all tumor CD8⁺ T cells (gray) and highlighting cells of control (292 cells) and SRF114 (1098 cells) treatment conditions. **G)** Percent frequency of CD8⁺ T cell clusters after each treatment condition. **H)** Dot heatmap showing activation-induced inhibitory receptors, effector function, and transcription factor genes within each CD8⁺ T cell cluster per treatment condition.

A) MC38 tumors were collected on Day 10 after implantation and hCCR8 expression was detected on Foxp3⁺ Treg cells by flow cytometry. B) Tumor size was measured over time after mice were dosed with SRF114 or control antibodies (n = 10). C) MC38 tumors were dissociated and Treg cell frequency was quantified by flow cytometry (n = 5). D-H) CD45⁺ TILs were isolated on Day 6 after treatment with SRF114 or control antibodies and transcriptome analysis was performed using 10X Genomics (n = 2-3 replicates, 5 pooled tumors per replicate).

Anti-CCR8 Therapy Results in Robust Anti-Tumor Activity and Depletion of Tumor Tregs, While Preserving Peripheral Treg Cells

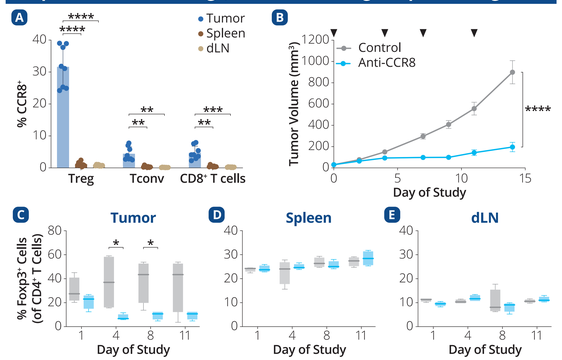

A) CCR8 expression in T cell subsets in dissociated CT26 tumors, spleen, and draining lymph nodes (dLN) on Day 14 post-implantation. **B)** Efficacy study in CT26 tumor model comparing anti-CCR8 to control antibody treatment. **C-E)** Cytometry analysis of Treg cell frequency in tumor, spleen, and dLN, respectively.

A) Dissociated tissues were collected from untreated mice and analyzed by flow cytometry (n = 8). B) Tumor volume was measured after dosing with anti-CCR8 or control antibodies (n = 10). C-E) Tissues were dissociated and analyzed by flow cytometry. Treg cells were gated as live CD45⁺, TCRβ⁺, CD4⁺, Foxp3⁺ cells, (n = 4).

Anti-CCR8 Therapy Impacts the Myeloid Cell Compartment and Increases its Maturation State

Cytometric analysis of the myeloid cell compartment in dissociated CT26 tumors on Day 11 after treatment with anti-CCR8 or control antibody. **A)** Cell frequency of each subset and **B-C)** changes in the expression of co-stimulatory molecules CD86 and CD80 in each myeloid cell subset, expressed as Fold-Change (anti-CCR8/Control, n = 4).

Conclusions

Mechanism of Action: SRF114 or Anti-CCR8 therapies Promote Depletion of Tumor CCR8⁺ Tregs and Reshape the TME Towards a Pro-inflammatory phenotype

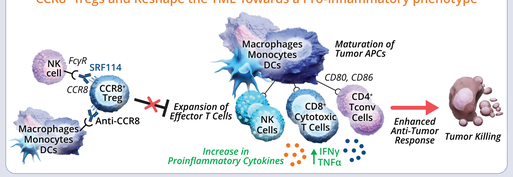

- Anti-CCR8 therapy depletes a subset of suppressive tumor Tregs, resulting in robust anti-tumor activity in multiple tumor models, including checkpoint inhibitor-resistant tumors.
- Anti-CCR8 therapy promotes expansion of tumor cytotoxic T cells and NK cells, and remodeling and maturation of the myeloid compartment.
- Anti-CCR8 and anti-PD-1 combination therapy improves overall survival in a checkpoint inhibitor-resistant melanoma model by promoting expansion of effector T cells and increasing pro-inflammatory cytokines and chemokines in the TME.
- SRF114, a fully human antibody targeting hCCR8, confers robust anti-tumor activity and reshapes the TME towards a proinflammatory state in hCCR8KI mice. SRF114 is currently being evaluated in Phase 1 clinical trials (NCT05635643).

Presented at AACR 2023